Expression and function of an *even-skipped* homolog in the leech *Helobdella robusta*

Mi Hye Song*, Françoise Z. Huang, Gwendolen Y. Chang and David A. Weisblat†

Department of Molecular and Cell Biology, University of California, 385 LSA, Berkeley, CA 94720-3200, USA
*Present address: Department of Molecular, Cellular and Developmental Biology, University of Michigan, Ann Arbor, MI 48109-1048, USA
†Author for correspondence (e-mail: weisblat@uclink4.berkeley.edu)

SUMMARY

We have identified homologs of the *Drosophila* pair-rule gene *even-skipped* in the glossiphoniid leeches *Helobdella robusta* and *Theromyzon trizonare*. In leech embryos, segments arise sequentially from five pairs of embryonic stem cells (teloblasts) that undergo iterated divisions to generate columns (bandlets) of segmental founder cells (primary blast cells), which in turn generate segmentally iterated sets of definitive progeny. In situ hybridization revealed that *Hro-eve* is expressed in the teloblasts and primary blast cells, and that these transcripts appear to be associated with mitotic chromatin. In more advanced embryos, *Hro-eve* is expressed in segmentally iterated sets of cells in the ventral nerve cord. Lineage analysis revealed that neurons expressing *Hro-eve* arise from the N teloblast.

To assess the function of *Hro-eve*, we examined embryos in which selected blastomeres had been injected with antisense *Hro-eve* morpholino oligonucleotide (AS-*Hro-eve* MO), concentrating on the primary neurogenic (N teloblast) lineage. Injection of AS-*Hro-eve* MO perturbed the normal patterns of teloblast and blast cell divisions and disrupted gangliogenesis. These results suggest that *Hro-eve* is important in regulating early cell divisions through early segmentation, and that it also plays a role in neuronal differentiation.

Key words: Leech, *even-skipped*, Segmentation, Annelid, Antisense oligonucleotides

INTRODUCTION

The evolutionary origin(s) of segmentation in bilaterally symmetric animals is a topic of interest and controversy (Davis and Patel, 1999). Until relatively recently, a mainstream view of this topic was that segmentation arose independently at two points in evolution: once in the deuterostome ancestor of the chordates, and once in the protostome ancestor of annelids, arthropods and onychophorans. Paradoxically, recent discoveries in comparative development and in molecular phylogeny have been interpreted as supporting two different and mutually contradictory scenarios. On one hand, the discovery that vertebrate homologs of *Drosophila* segmentation genes are expressed in segmentally iterated patterns has led some to propose that the last common ancestor of protostomes and deuterostomes was already segmented (De Robertis, 1997; Holland et al., 1997; Kimmel, 1996). On the other hand, molecular phylogenies now organize most or all bilaterians into three clades, Deuterostomia, Ecdysozoa and Lophotrochozoa (Aguinaldo et al., 1997; Ruiz-Trillo et al., 1999), that have been evolving separately since before the Cambrian radiation (Adoutte et al., 2000). As each of these clades contains only a minority of segmented taxa (Brusca and Brusca, 1990), it is more parsimonious to conjecture that segmentation evolved independently in each of the three clades.

Analyzing the mechanisms of segmentation in glossiphoniid leeches such as *Helobdella robusta* may contribute to resolving this paradox by either of two routes. For example, finding that segmentation is homologous between leeches (a highly derived but experimentally tractable taxon of segmented lophotrochozoans) and insects (a highly derived but experimentally tractable taxon of segmented ecdysozoans) would suggest that the urprotostome was already segmented, and would be consistent with the hypothesis that the urbilaterian was already segmented as well. Conversely, concluding that segmentation is not homologous between representatives of the two clades of protostomes would support the hypothesis that segmentation arose multiple times.

The primary pair-rule gene *even-skipped* (*eve*) is among the first genes to exhibit regular, spatially iterated patterns in *Drosophila* (Frasch et al., 1987; Macdonald et al., 1986). Homologs of *eve* have also been described in arthropods, such as the beetle *Tribolium castaneum* and the grasshopper *Schistocerca americana*, and the spider *Cupiennius salei*, that form segments sequentially. *Tribolium-eve* and *Cupiennius-eve* are expressed in striped patterns that correlate with segmentation (Brown et al., 1997; Damen et al., 2000; Patel, 1994), while *Schistocerca-eve* is expressed in the posterior growth zone without forming stripes (Patel et al., 1992). Neuronal expression of *eve*-class genes is conserved throughout the arthropods (Damen et al., 2000; Duman-Scheel and Patel, 1999; Frasch et al., 1987; Patel et al., 1992).

We report the identification of *eve*-class genes from two species of glossiphoniid leeches and the initial characterization of *Hro-eve*, the *eve* homolog in *Helobdella robusta*. Semi-quantitative RT-PCR revealed that the highest levels of *Hro-eve* transcription occur during organogenesis. In situ hybridization revealed earlier expression, during cleavage and the early phases of segmentation, but we found no evidence for a pair-rule pattern. In early development, *Hro-eve* transcripts seem to be associated with mitotic chromatin in the stem cells of the posterior growth zone (teloblasts) and in their progeny (primary blast cells) that are the founder cells for the five distinct lineages of segmental mesoderm and ectoderm. In more advanced embryos, *Hro-eve* is expressed in segmentally iterated subsets of the neurons that arise from the N teloblasts. To assess the function of *Hro-eve*, we examined embryos in which selected blastomeres had been injected with antisense *Hro-eve* morpholino oligonucleotides (AS-*Hro-eve* MO). Focussing on the N lineage, we found that teloblasts injected with AS-*Hro-eve* MO continued to divide at about the normal rate, but other aspects of their division were disturbed, and primary blast cell divisions were also disrupted. Presumably because of these early effects on teloblasts and blast cells, segmentation was also perturbed in the injected lineage, as evidenced by misalignment of left and right hemiganglia, fusion of serially adjacent hemiganglia and/or missing groups of cells. Ganglionic neurons expressing *Hro-eve* arose, though in an abnormal pattern; serotonergic neurons failed to form. In the O lineage, injection of AS-*Hro-eve* MO disrupted both neural and epidermal cell fates. Our results suggest that *Hro-eve* is important in regulating cell divisions in stem cells and segmental founder cells in early development and that it also regulates the differentiation of a subset of ganglionic neurons. However, we find no evidence that *Hro-eve* plays a pair rule function similar to that of *eve*-class genes in arthropod segmentation.

MATERIALS AND METHODS

Embryos

Embryos of *Helobdella robusta* were obtained from a laboratory colony and those of *Theromyzon trizonare* from specimens collected in the ponds of Golden Gate Park, San Francisco, and cultured at 23°C in HL (Helobdella) saline (Blair and Weisblat, 1984). The embryonic staging system and cell nomenclature are as reviewed elsewhere (Fig. 1) (Weisblat and Huang, 2001).

Microinjections

To mark specific cell lines, cells were pressure injected with rhodamine-conjugated dextran amine (RDA, Molecular Probes, catalog number D-1827) or fluorescein-conjugated dextran amine (FDA, Molecular Probes, catalog number D-1820) at a final concentration of 75 mg/ml in 0.2 N KCl with 1% Fast Green as described previously (Smith and Weisblat, 1994).

To perturb *Hro-eve* expression, cells of interest were injected with an antisense morpholino oligonucleotide (MO; Genetools) complementary to the downstream end of the 5′ UTR and first five bases of coding sequence of *Hro-eve*, designated as AS-*Hro-eve* MO (5′-AT<u>CAT</u>TTTACTTTTCGATTCAGCGG-3′; anti-start codon underlined). For control injections, we used a generic MO (5′-CCTCTTACCTCAGTTACAATTTATA-3′) or MM-*Hro-eve* MO (5′-ATCtTTTaACTTTTCGATaCAGgGG-3′) that had the same overall nucleotide composition as AS-*Hro-eve* MO, but with four mismatched nucleotides (Nasevicius and Ekker, 2000).

MO concentrations ranged from 0.06-1.3 mM in the micropipette and the volume of material injected corresponds to roughly 1% of the teloblast (Bissen and Weisblat, 1987). Thus, we estimate that the MO concentrations ranged from 0.6-13 μM in the cytoplasm of the injected cells. MO was co-injected with lineage tracer (~50 mg/ml in the pipette) and Fast Green (~0.5% in the pipette).

Gene isolation

Degenerate oligonucleotides (upstream, 5′-MGIYAYMGIACIGCITT-3′; downstream, 5′-YGIYAYYTTRTCYTTCAT-3′) corresponding to nucleotides 7-24 and 108-125 of the *eve*-class homeobox were designed by comparing the sequences for *eve*-class genes from zebrafish (Joly et al., 1993), fly (Macdonald et al., 1986), mouse (Bastian and Gruss, 1990), human (Faiella et al., 1991), coral (Miles and Miller, 1992), grasshopper (Patel et al., 1992), nematode (Ahringer, 1996) and frog (Ruiz i Altaba and Melton, 1989). Candidate gene fragments were amplified from a cDNA library (Stratagene) of stage 7-10 embryos by degenerate PCR.

To obtain additional sequence of *Hro-eve*, we performed PCR on the cDNA library and on first strand cDNAs. For the first strand cDNA, ~500 embryos from stages 6-10 were homogenized in RNAwiz (Ambion) and total RNA was extracted. Polyadenylated mRNAs were isolated using Oligotex mRNA mini kit (Qiagen). For rapid amplification of the cDNA ends, the Marathon cDNA amplification kit (Clontech) was used, with exact gene specific oligos designed from the gene fragments described above. Sequence analyses were performed by the MacDNASIS pro v3.5 program and the BLAST program (http://www.ncbi.nlm.nih.gov).

Semi-quantitative developmental RT-PCR

At each stage, total RNAs were extracted from 50 embryos and treated with DNase (DNA-free, Ambion), and then reverse-transcribed using random decamers (Ambion). As an internal standard to adjust for differences in efficiency of RNA extraction between samples, a 488 bp fragment of 18S rRNA was amplified in parallel to each sample. To quantitate PCR products, each sample was electrophoresed in 2% agarose gel and stained with ethidium bromide. Band intensity was measured with an Alphaimager (Alpha Innotech) using Alphaease (v3.3b) program.

To confirm the relative levels of expression, we amplified two separate regions of *Hro-eve* cDNA: nucleotides 784-1243 (which spans an intron site, to control for the possibility of genomic DNA contamination of the template) and nucleotides 1724-1939. Both produced equivalent results, and the identity of the amplified fragments was confirmed by sequencing one sample of each fragment.

In situ hybridization

Digoxigenin (Dig-11-UTP, Roche)-labeled riboprobes were made in vitro using MEGAscript kit (Ambion) and hydrolyzed. T7 RNA polymerase (Ambion, cat No. 1334) was used for all probes. Sequence for *Hro-eve* riboprobes includes 3′ coding region and most of the 3′-UTR (nucleotides 1211-3140).

To localize *Hro-eve* mRNA in situ, two different protocols were used, depending on the age of the embryo. Embryos at stages 9-11 were processed as described previously (Harland, 1991; Nardelli-Haefliger and Shankland, 1992). For early stages (through stage 8), embryos were fixed in 4% formaldehyde, 1×phosphate-buffered saline (PBS, diluted from 10× PBS stock, pH 7.4) for 1 hour at room temperature. After fixation, all incubations were performed at room temperature with constant rocking. Fixed embryos were rinsed with 0.1% PBTw (PBS, 0.1% Tween 20), devitellinized and rinsed in serial changes of 0.1% PBTw, 0.1% PBTw:HYB (1:1) and hybridization solution [HYB; 5×SSC, tRNA 0.5 mg/ml, heparin 50 μg/ml, 0.1% Tween 20, 50% formamide, pH 6.0 (adjusted with 1 M citric acid)], then pre-hybridized in HYB for 2 hours at 68°C. HYB was replaced with fresh HYB containing riboprobes and hybridized at 68°C for 28-40 hours. Embryos were washed with pre-warmed HYB:2×SSC/0.3%
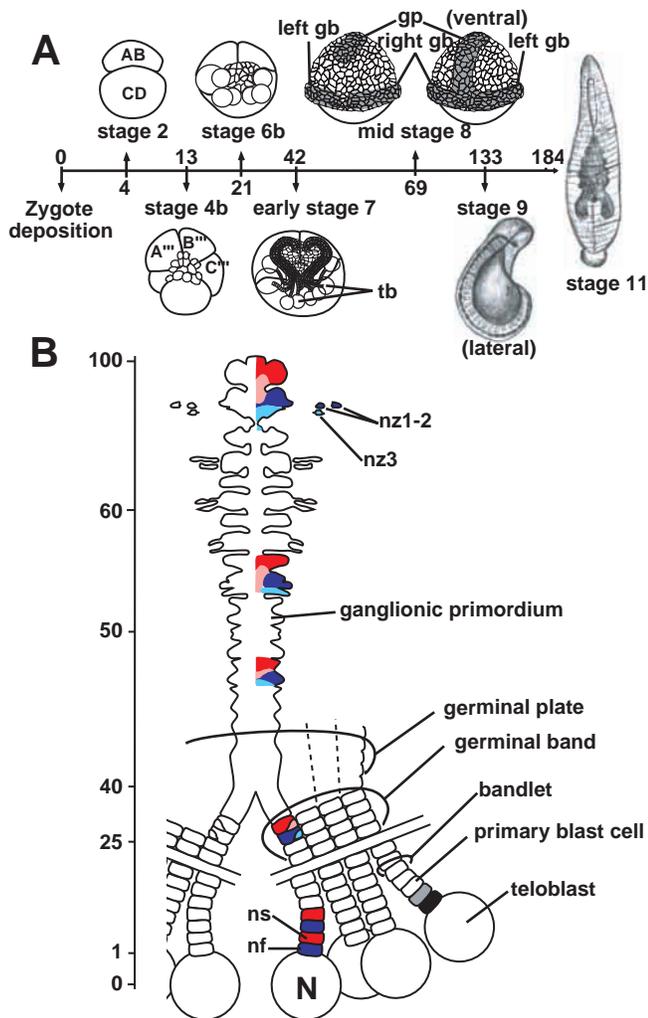
Fig. 1. Summary of *Helobdella* development. (A) Timeline (not to scale) showing selected developmental stages; all views are from the animal pole (prospective dorsal) unless indicated otherwise. Times given indicate the approximate age in hours after zygote deposition at 23°C. tb, teloblast; gb, germinal band; gp, germinal plate. (B) The formation of segmental ectoderm, focussing on the N lineage. Each N teloblast undergoes stem cell divisions to produce primary ns (red) and nf (dark blue) blast cells in exact alternation. The timing of subsequent events in each n blast cell clone is given in terms of the time elapsed since the birth of the primary blast cell (hours clonal age; timeline not to scale). Ipsilateral columns (bandlets) of primary blast cells merge to form germinal bands, which coalesce in anteroposterior progression during stage 8 into the germinal plate, from which segments arise (see A). The ns and nf blast cells undergo distinct and stereotyped lineages, beginning with unequal, obliquely anteroposterior divisions producing progeny called ns.a (red), ns.p (pink), nf.a (dark blue) and nf.p (light blue) at ~28 and ~26 hours clonal age, respectively. During subsequent development, these subclones generate approx. two-thirds of the ~200 identified neurons and glia in each hemiganglion, plus three peripheral neurons (nz1-3) and a few epidermal cells (not shown) (Bissen and Weisblat, 1987; Bissen and Weisblat, 1989; Kramer and Weisblat, 1985; Ramirez et al., 1995; Shain et al., 1998; Shain et al., 2000; Weisblat et al., 1984; Zackson, 1984).

conjugated goat anti-rabbit (1:300, Jackson ImmunoResearch Labs 111-036-003, West Grove, PA) overnight at 4°C. Embryos were rinsed in PTN, then in PBS and incubated in 0.75×PBS containing 0.5 mg/ml 3, 3′-diaminobenzidine (Sigma) and 0.008% $NiCl_2$ for 15 minutes at room temperature. The color reaction was initiated by adding 0.06% H_2O_2 and monitored visually. For observation, germinal plates were dissected and mounted in ~75% glycerol.

Histology and microscopy

For more detailed analyses, selected embryos were sectioned prior to microscopic examination. For this purpose, embryos labeled with lineage tracer only were dehydrated and embedded in glycol methacrylate resin (JB-4, Polysciences) according to the manufacturer's instructions. This resin dissolves the colored in situ hybridization reaction product. Thus, in situ-stained embryos were embedded in an epoxide resin (Polybed 812, Polysciences). Embedded embryos were sectioned at ~10 µm thickness (MT2-B Ultramicrotome, Sorvall) and mounted on glass slides using a non-fluorescent media (Fluoromount, BDH Laboratory Supplies, England). Intact, dissected or sectioned embryos were examined and photographed with DIC and/or epifluorescence optics (Zeiss Axiophot and 35 mm film camera or Nikon E800 and Princeton Instruments cooled CCD camera controlled by UIC Metamorph software) or by confocal microscopy (BioRad MRC 1024). Images were processed, montaged and composed digitally (Metamorph, UIC; Photoshop 5.0, Adobe).

chaps (1:1), and then 2×SSC/0.3% Chaps, followed by successive 20 minute washes with 2×, 0.2× and 0.1× SSC/0.3% Chaps at 68°C. Embryos were incubated in blocking solution [0.1% PBTw, 2% sheep serum (Sigma, St Louis, MO), 2 mg/ml bovine serum albumin] for 2 hours at room temperature and further incubated in blocking solution containing anti-digoxigenin alkaline phosphatase-conjugated polyclonal Fab fragments (1:5000, Roche) at 4°C overnight. Embryos were rinsed with frequent changes of 0.1% PBTw for 5 hours at room temperature, followed by a brief rinse with alkaline phosphatase buffer (AP buffer; 100 mM Tris-HCl, pH 9.5, 100 mM NaCl, 50 mM $MgCl_2$, 0.1% Tween 20). Embryos were then incubated in AP buffer containing 4-nitro blue tetrazolium chloride/5-bromo-4-chloro-3-indoyl-phosphate (Roche) for color reaction. When the embryos reached the desired color, they were rinsed with double distilled H_2O and dehydrated in a graded ethanol series, then cleared in benzyl benzoate:benzyl alcohol (3:2) for observation.

Anti-serotonin staining

Embryos at stage 11 were fixed in 4% formaldehyde in 0.75×PBS overnight at 4°C and washed in 1×Hepes-buffered saline (HBS, diluted from 2×stock), then incubated for 24 hours in HBS containing 0.5 units/ml chitinase (Sigma C-1525, St Louis, MO) at RT with gentle shaking. Embryos were rinsed in HBS and incubated in a solution of PBS, 1% Triton X-100 and 10% NGS (PTN) overnight at 4°C, then further incubated in PTN containing rabbit anti-serotonin (1:300, Sigma S-5545, St. Louis, MO) overnight at 4°C. Embryos were rinsed in PTN and incubated in PTN containing peroxidase-

RESULTS

Identification of *eve*-class genes from glossiphoniid leeches

Using degenerate PCR, we amplified fragments of the homeobox of *eve*-class genes from *Helobdella robusta* and *Theromyzon trizonare*, then used 5′- and 3′-RACE on the cDNA library and first strand cDNAs to obtain additional sequence for these genes, designated *Hro-eve* (Accession Number, AF409098) and *Ttr-eve* (Accession Number, AY050275), respectively. The homeodomains of *Hro-eve* and *Ttr-eve* show

Fig. 2. (A) Comparison of *eve*-class homeodomain sequences from lophotrochozoans (Hro, *Helobdella robusta*; Ttr, *Theromyzon trizonare*), cnidarians (Afo, *Acropora formosa*; Nve, *Nematostella vectensis*), deuterostomes (Bfl, *Branchiostoma floridae*; Dre, *Danio rerio*; Mmu, *Mus musculus*; Hsa, *Homo sapiens*; Xla, *Xenopus laevis*) and ecdysozoans (Cel, *Caenorhabditis elegans*; Dme, *Drosophila melanogaster*; Sam, *Schistocerca americana*; Tca, *Tribolium castaneum*). Two similar non-*eve*-class homeodomain sequences are included for comparison (HmHD, *Hirudo medicinalis* homeodomain protein; Dmpb, *Drosophila melanogaster proboscipedia*). Consensus amino acid residues are highlighted, and amino acid residues flanking known intron sites are underlined. Values in parentheses indicate the percentage amino acid identity with *Hro-eve*.

	HELIX1	HELIX2	HELIX3	HELIX4	
Hro	LRRYRTAFTREQLAK	LEKEFLKENYVSRPRRCELASQLDLPECTI	KVWFQNRRMKDKRQR		(100%)
Ttr	MKRYRTAFTRDQLNKL	EQEYQRETYVSRPRRSELAATLNLPDSTI	KIWFQNRRMKDKRQR		(73%)
Dme	VRRYRTAFTRDQLRLE	KEFYKENYVSRPRRCELAAQLNLNLPESTI	KVWFQNRRMKDKRQR		(86%)
Sam	IRRYRTAFTREQLARL	EKEFYKENYVSRPRRCELASQLNLPESTI	KVWFQNRRMKDKRQR		(91%)
Tca	IRRYRTAFTREQLARL	EKEFFKENYVSRPRRCELAAQLNLPESTI	KVWFQNRRMKDKRQR		(90%)
Dre	SRRHRTAFTREQLTRL	EQEYCKESYVSRPRRCELAAALNLPETTI	KIWFQNRRMKDKRQR		(81%)
Hsa	MRRYRTAFTREQIARL	EKEFYRENYVSRPRRCELAAALNLPETTI	KVWFQNRRMKDKRQR		(85%)
Mmu	MRRYRTAFTREQIARL	EKEFYRENYVSRPRRCELAAALNLPETTI	KVWFQNRRMKDKRQR		(85%)
Xle	MRRYRTAFTREQIARL	EKEFYRENYVSRPRRCELAAALNLPETTI	KVWFQNRRMKDKRQR		(85%)
Cel	MRRYRTAFSREQIGRL	EREFAKENYVSRKTRGELAAELNLPEGTI	KVWFQNRRMKDKRQR		(76%)
Nve	TRRYRTAFTREQLKRL	EKEFMRENYVSRTRRCELANALNLSETTI	KIWFQNRRMKSKRRR		(77%)
Afo	TRRYRTAFTREQLSRL	EKEFLRENYVSRPRRCELANALNLPETTI	KVWFQNRRMKDKRQR		(85%)
Bfl	VRRYRTAFTREQLARL	EKEFRENYVSRPRRCELAAQLNLPETTI	KVWFQNRRMKDKRQR		(88%)
HmHD	NKRTRTAYSRAQLLE	LEKEFHYDKYISRPRRLELAASLNLTERHI	KIWFQNRRMKWKKLE		(59%)
Dmpb	PRRLRTAYTNTQLLE	LEKEFHFNKYLCRPRRIEIAASLDLTERQY	KVWFQNRRMKHKRQT		(63%)

73-91% amino acid identity with those of other *eve*-class genes (Fig. 2); the closest non-*eve*-class homeodomain is from *Drosophila proboscipedia*, with 63% identity. Thus, we are confident that these genes are bona fide *eve*-class genes.

The ~1.4 kb of *Ttr-eve* cDNA sequence encodes a polypeptide of at least 421 amino acids. There is no in frame stop codon in the 96 bp of 5′ sequence prior to the first methionine in the ORF and no polyadenylation signal in the 59 bp of 3′-UTR. The sequence was confirmed by comparison with genomic DNA, which revealed a 269 bp intron within the homeodomain, following amino acid residue 46 of the homeodomain. This intron site is conserved in mouse, human, frog, nematode and *Tribolium* (Fig. 2) (Ahringer, 1996; Bastian and Gruss, 1990; Brown et al., 1997; Faiella et al., 1991; Ruiz i Altaba and Melton, 1989).

For *Hro-eve*, ~3.1 kb of cDNA was obtained, encoding an ORF of at least 761 amino acids, taking the 5′-most in frame AUG as the start codon. There was no in-frame stop codon in the 171 bp upstream of the candidate start codon; three possible polyadenylation sites occurred in the 676 bp of 3′-UTR. In addition to the homeodomain, the *Hro-eve* polypeptide contains a polyalanine stretch and another region rich in serine and proline residues, both of which are common features in other *eve*-class genes (Ahringer, 1996; Bastian and Gruss, 1990; Brown et al., 1997; Faiella et al., 1991; Macdonald et al., 1986; Patel et al., 1992; Ruiz i Altaba and Melton, 1989). Comparison with genomic DNA revealed one 257 bp intron at the same site within the homeodomain as in other *eve*-class genes and another, 100 bp intron following amino acid residue 51 of the putative polypeptide.

To compare *Ttr-eve* and *Hro-eve* to other *eve*-

class genes, cladograms were constructed [PAUP 4.0 b4a (PPC)] using only homeodomains. Both *Ttr-eve* and *Hro-eve* clearly fell within a strongly supported clade of *eve*-class genes (98% bootstrap value), but there was no well-supported resolution within this clade (data not shown but available upon request). *Ttr-eve* and *Hro-eve* showed less amino acid identity than expected for orthologous genes from closely related species (Fig. 2) and were highly diverged outside the homeodomain. These results could reflect either an ancient duplication of the protostome *eve*-class gene or the rapid divergence of the *Ttr-eve*; we cannot distinguish between these possibilities. In any event, for the following analyses of gene expression and function, we focussed exclusively on *Hro-eve*.

Hro-eve is not expressed in a pair rule pattern during segmentation

In *Helobdella*, each segment arises from the interdigitating clones of seven distinct classes of bilaterally paired segmental founder cells (m, nf, ns, o, p, qf and qs blast cells) (reviewed by Weisblat and Huang, 2001) (Fig. 1). Blast cells arise in columns (bandlets) by unequal divisions from five bilateral pairs of large identified stem cells: the M, N, O, P and Q teloblasts. Teloblasts divide with a cell cycle time of about 1

Fig. 3. Semi-quantitative RT-PCR analysis of *Hro-eve* expression. Ethidium bromide-stained gels (below) show *Hro-eve* and 18S rRNA bands from various developmental stages (0 denotes oocyte; e, early). The extent of amplification (23 cycles for 18S rRNA and 30 cycles for *Hro-eve*) was chosen empirically to avoid saturation of the amplified bands. The graph (above) shows the average of the intensity of the *Hro-eve* bands after normalizing by the intensity of the corresponding 18S rRNA band and plotting relative to stage 10, from five different experiments. Error bars indicate the standard deviation of the mean.
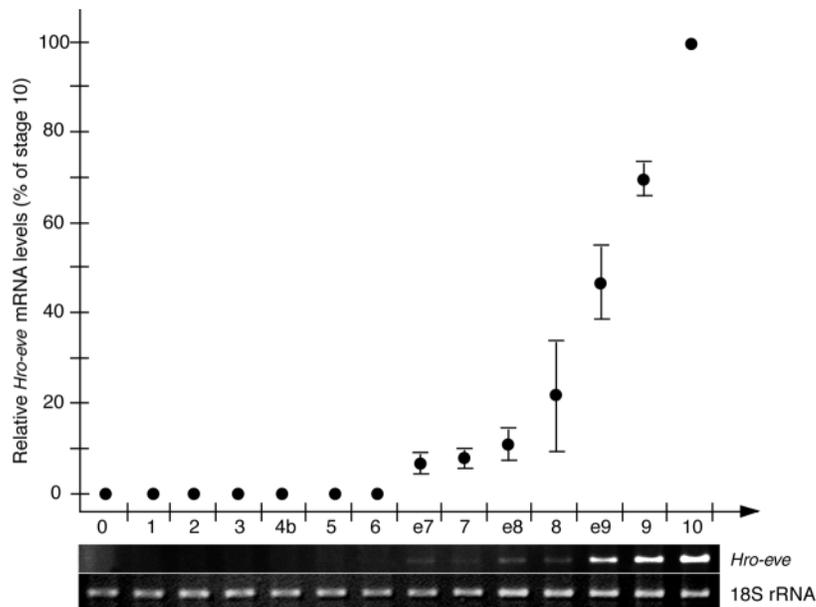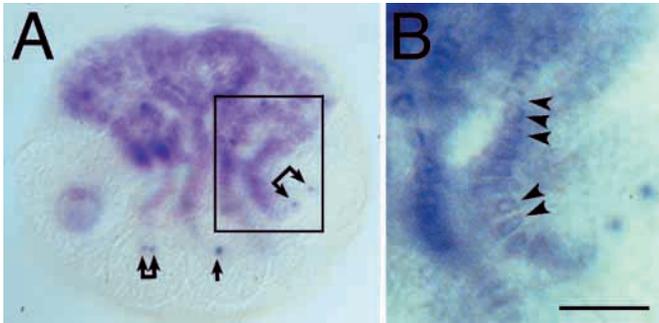
Fig. 4. Early expression of *Hro-eve* provides no evidence for pair rule patterning. (A) Bright-field (Nomarski optics) image of a stage 7 embryo processed by in situ hybridization for *Hro-eve*. Staining is uniform within and among bandlets, except for punctate staining associated with apparent mitotic figures in three teloblasts; arrow indicates prophase; yoked arrows indicate telophase (left) and anaphase (right). An enlarged view (B) at a slightly different focal plane of the outlined region of the same embryo shows perinuclear staining of *Hro-eve* in blast cells of the bandlets (arrowheads), but no alternating intensity of staining that would be indicative of a pair-rule expression pattern. Scale bar: 100 μm in A; 30 μm in B.

hour. Each lineage contributes a stereotyped set of neurons and other cell types to each segment. In the N (and Q) lineages, two classes of blast cells, nf and ns (qf and qs) arise in exact alternation; one of each is required to generate one segment's worth of progeny (Fig. 1). In the M, O and P lineages, each blast cell makes one segment's worth of progeny. In each teloblast lineage, the first-born blast cells contribute to anterior segments and blast cells born later contribute to progressively more posterior segments.

Thus, in leech, in contrast to vertebrates and insects, there is a strict correlation between the 'cell cycle clock', by which blast cells arise from the teloblasts, and the 'segmentation clock', by which segmental tissues arise in anteroposterior progression. From this description, what might one expect to see if *Hro-eve* was expressed in a pair-rule pattern? One possibility was that *Hro-eve* would be expressed in alternate blast cells, or blast cell clones, in the M, O and P lineages, and in alternate pairs of blasts cells in the N and Q lineages.

Another possibility was that it would be expressed in alternate cells within the N and Q lineages, for example, in all nf and qf cells.
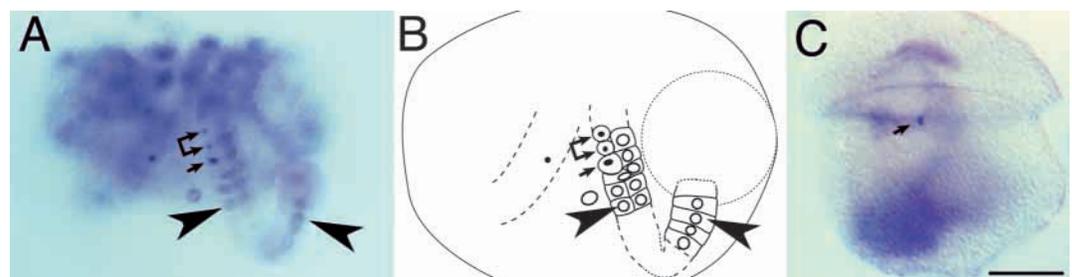
As a first step in characterizing the expression of *Hro-eve*, we used semi-quantitative RT-PCR to estimate the relative levels of expression of *Hro-eve* during development (Fig. 3). By this technique, *Hro-eve* transcripts were present in embryos at stage 7, which roughly corresponds to the onset of blast cell production. But in contrast to predictions based on pair-rule expression patterns, in situ hybridization of embryos at stages 7-8 revealed *Hro-eve* mRNA in all primary blast cells and in the micromere cap (Fig. 4A). The level of staining was uniform among different lineages, and among individual blast cells within each bandlet (Fig. 4A,B). Thus, we found no evidence for either lineage-specific or pair rule expression of *Hro-eve*.

In early development, *Hro-eve* transcripts were associated with chromatin of mitotic cells

In these experiments, some teloblasts in each embryo exhibited punctate staining that resembled chromatin morphology during mitosis (Fig. 4). These features suggested that *Hro-eve* transcripts had colocalized with the chromatin of mitotic teloblasts. We were unable to obtain nuclear counterstaining under the conditions for in situ hybridization process, but punctate staining also occurred within bandlets and germinal bands at the specific positions where primary blast cells undergo mitosis (Bissen and Weisblat, 1987; Zackson, 1984). This pattern of chromatin staining was most easily seen in the mesodermal (m) bandlet because m blast cells undergo their first two divisions prior to entering the germinal bands (Fig. 5A,B).

The specificity of this chromatin staining was confirmed by control experiments. Experiments using both sense probe for *Hro-eve* and no probe gave no staining (data not shown). By contrast, in situ staining for other *Helobdella robusta* genes gave distinct patterns: *Hro-nos* (a *nanos* homolog) (Pilon and Weisblat, 1997; Kang et al., 2002) gave very faint, diffuse staining; *Hro-cycA* (a *cyclinA* homolog) (Chen and Bissen, 1997) gave strong cytoplasmic staining in teloblasts and blast cells (data not shown). Thus, we conclude that the *Hro-eve* in situ signal represented an association of *Hro-eve* transcripts with the chromatin of teloblasts and blast cells during mitosis.

Fig. 5. Early *Hro-eve* transcripts appear to be associated with chromatin of cells in mitosis. Brightfield (Nomarski optics) images of embryos processed by in situ hybridization for *Hro-eve*. (A) Ventral view of a stage 7 embryo. On the right, regions of an m bandlet are in focus. The M teloblast is out of focus, but ~4 m blast cells in the proximal bandlet (one cell wide because the primary blast cells have not yet divided) are in view. Distal to this, the bandlet is in focus again, now two cells wide; in each pair of secondary m blast cells, m.l is on the left and m.m is on the right; perinuclear localization of the *Hro-eve* transcripts in the blast cells can be seen, as in Fig. 4 (arrowheads). Cell m.l divides prior to m.m in *Helobdella* (Bissen and Weisblat, 1989) (E. K. Schimmerling, BA Honors thesis, University of California, 1986). In this embryo, the in situ signal in successive m.l cells is punctate instead of perinuclear, which corresponds to the younger cell (arrow) in prophase, and the older cell (yoked arrows) in telophase. The other m bandlet is largely out of focus, but one m.l in that bandlet exhibits punctate staining. (B) Schematic drawing of the embryo in A. (C) In a late two-cell embryo, punctate staining (arrow) marks the metaphase chromatin of cell CD. Diffuse background staining of teloplasm is also evident. Scale bar: 100 μm.
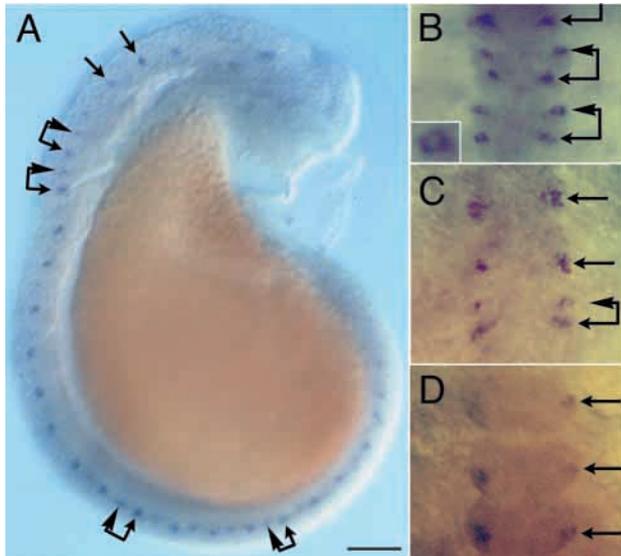
Fig. 6. Dynamic pattern of late *Hro-eve* expression in ganglionic neurons. Bright-field (Nomarski optics) images of embryos processed by in situ hybridization for *Hro-eve*. (A) Lateral view of a stage 9 embryo. In anterior, developmentally advanced segments, the spots of *Hro-eve* expression show segmental periodicity (arrows), while in posterior, less advanced segments, there are two spots per segmental repeat (yoked arrowheads and arrows). (B-D) Ventral views of anterior midbody ganglia (~M2-M5) at three different stages; note that these *Hro-eve* transcripts exhibit cytoplasmic localization; transcripts are excluded from nuclei. (B) At mid stage 9, there are distinct anterior and posterior spots of expression in each hemiganglion (yoked arrowheads and arrows, respectively). Inset: enlarged image of the adjacent cell shows cytoplasmic staining and unstained nucleus. (C) By late stage 9, anterior expression has ceased in anterior segments, whereas the posterior spot is still present in all three segments. (D) By late stage 10, anterior expression is completely gone, but the posterior spots (arrows) remain. Scale bar: 100 μm in A; 50 μm in B-D; 20 μm in inset.

We did not examine all the stages during cleavage, but similar staining was seen as early as the two-cell stage (Fig. 5C), indicating that *Hro-eve* is expressed throughout cleavage at levels beneath the sensitivity of our RT-PCR protocol.

Late expression of *Hro-eve* was in subsets of developing neurons

RT-PCR experiments indicated that *Hro-eve* expression increased sharply beginning in stage 9, by which time the germinal plate is complete and the differentiation of ventral ganglia and other segmental tissues is under way. In situ hybridization using embryos at stages 9-11 revealed *Hro-eve* expression in segmentally iterated sets of neurons in the ventral nerve cord (Fig. 6). The *Hro-eve* transcripts in these cells were cytoplasmic rather than nuclear (Fig. 6).

Two lines of evidence showed that neuronal *Hro-eve* expression was dynamic over time, and that it undergoes the same progression in each of the midbody segments. First, within individual embryos, there were differences in staining pattern along the AP axis that correlate with the sequential segmentation process in leech (Fig. 6A). Second, the same changes in *Hro-eve* expression were seen by examining any given region of the germinal plate at progressively later stages

of development (Fig. 6B-D). Thus, the following description applies to any midbody ganglion and is presented in terms of the clonal age of the n blast cells that contribute to the ganglion, as neurons expressing *Hro-eve* arise from the nf and ns blast cells (see below).

Neuronal expression of *Hro-eve* was first observed when n blast cell clones were ~70 hours old. This corresponds to early stage 9 in the anterior germinal plate. Expression was seen in two spots, one anterior and another more posterior, in each hemiganglion (Fig. 6B). The anterior spot consisted of two or three adjacent cells in the ventrolateral portion of the ganglion; the more posterior spot lies about halfway back in the ganglion and consists of two or three cells in the dorsal portion of the ganglion, roughly midway between the ventral midline and the lateral edge of the ganglion. By clonal age ~90-100 hours, the anterior spot of *Hro-eve* expression started to disappear, so that some ganglia had only one anterior spot (Fig. 6C). By clonal age ~130 hours, the anterior spots had disappeared, but the posterior spot of *Hro-eve* expression remained in each ganglion through clonal age ~130-150 hours. Therefore, the posterior spot was evident throughout the germinal plate in individual embryos at late stage 10 (Fig. 6D).

In glossiphoniid leeches, ganglionic neurons arise from each of the five teloblast lineages, with half or more arising from the N lineage (Kramer and Weisblat, 1985; Weisblat et al., 1984). To identify the lineage(s) of origin of the neurons expressing *Hro-eve*, we carried out in situ hybridization on embryos in which one or more cells (N, OP or OPQ) had been injected with lineage tracer. The confocal images of sectioned embryos revealed that the in situ label colocalized with lineage tracer when the N lineage was labeled and not when any other lineage was labeled (Fig. 7). Thus, we conclude that the cells expressing *Hro-eve* arose from the N teloblasts. Moreover, by comparison with more detailed lineage analyses (Shain et al., 1998), we concluded that anterior ventrolateral cells exhibiting transient expression of *Hro-eve* arose from the ns.a clone, and that the posterior neurons arose from the nf.a clone in each segment.

Injection of antisense *Hro-eve* oligonucleotide into N teloblasts disrupted gangliogenesis

The expression of *Hro-eve* in the teloblasts and primary blast cells suggested that this gene might be involved in some early aspects of segmentation. To investigate the developmental role of *Hro-eve*, we injected teloblasts with antisense or control MO (AS-*Hro-eve* MO and MM-*Hro-eve* MO, respectively), together with Fast Green and lineage tracer to monitor the injections and to follow the development of the injected cells, respectively. In most embryos, one teloblast was injected with AS-*Hro-eve* MO and the contralateral teloblast with lineage tracer alone, to monitor normal development, or in combination with a control MO. Here, we focussed primarily on the N teloblast lineage (Fig. 1).

We estimate that the MO concentrations ranged from 0.6-13 μM in the cytoplasm of the injected teloblasts. When AS-*Hro-eve* MO was injected into N teloblasts at lower concentrations, the overall pattern of development was normal until stage 10 (~140 hours after the injection). But fluorescence microscopy revealed marked abnormalities in the distribution of progeny from the experimental N teloblasts. The usual segmental pattern of RDA-labeled ganglionic neurons was disrupted and was often out of register with the control side (Fig. 8A-C). At
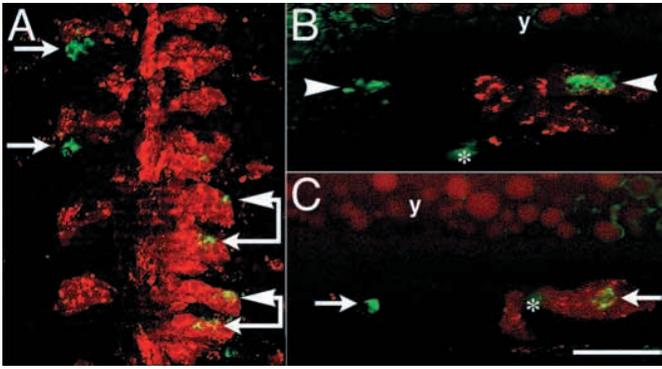
Fig. 7. Ganglionic cells expressing *Hro-eve* arise from the N lineage. Pseudo-colored confocal images of sectioned embryos that had been fixed and stained for *Hro-eve* transcripts (green) at stage 9 and in which 1 or more cells had been injected with RDA (red) at stage 6a. (A) A horizontal view of approx. four segmental ganglia in which the O, P and Q lineages are labeled on the left and the N lineage is labeled on the right. Anterior is upwards; the plane of section is oblique. In each hemiganglion, the posterior spot of *Hro-eve* expression lies just posterior to the main lobe of OPQ-derived cells (arrows) and in the anterior edge of the posterior half-ganglion (yoked arrows). The anterior spots of *Hro-eve* expression (yoked arrowheads) lie at the anterior edge of the ganglion. (B,C) Transverse sections through the ventral nerve cord of an embryo in which an N teloblast had been labeled; *Hro-eve*-positive neurons in the anterior spot (B, arrowheads) and posterior spot (C, arrows) colocalize with N-derived cells. Yolk platelets (y) exhibit background fluorescence in the RDA channel; background in situ signal is present between yolk platelets and imperfections in the sectioned material (*) also appear green in the pseudo-colored images. Scale bar: 50 μm in A; 30 μm in B,C.

higher concentrations, development was more severely perturbed; these embryos suffered higher than normal mortality during gastrulation (37/120 embryos died in six experiments), which was due to a failure of germinal plate formation and consequent rupture and leakage of the yolk cell. Many of the surviving embryos exhibited dorsolaterally directed hairpin loops in the posterior portion of the germinal plate (Fig. 9) that was not seen with control injections. Further analyses of this phenomenon are described later.

Injection of antisense *Hro-eve* oligonucleotide blocked neuronal differentiation

Two assays were used to assess the effects of AS-*Hro-eve* MO on specific neuronal phenotypes. For one, we used in situ hybridization for *Hro-eve* to mark the subsets of nf- and ns-derived neurons described above. Cells expressing *Hro-eve* arose from N teloblasts injected with AS-*Hro-eve* MO, but the pattern was abnormal; such cells were often out of register with their counterparts in the control half of the germinal plate (Fig. 8D,E). For another assay, we used immunostaining to screen for the appearance of three pairs of serotonergic neurons, the anteromedial giant Retzius neurons, which normally arise from the ns.a blast cell clones, and smaller ventrolateral and dorsolateral neurons (cells 21 and 61, respectively), which normally arise from nf.a clones (Stuart et al., 1987). These three neurons arose in their normal positions in control bandlets, but no serotonergic neurons were detected in the experimental bandlets (Fig. 8F).

Further examination of lineage tracer in cells derived from the experimental N teloblasts revealed that they had failed to generate appreciable numbers of neurites. In normal development, three prominent segmental nerves exiting each side of the ganglion (Ort et al., 1974; Stent et al., 1992), contain neurites derived from contralateral N-derived neurons (Shain et al., 1998); these nerves were not detected contralateral to AS-*Hro-eve* MO-injected N teloblasts, in contrast to the case with control injections (data not shown). Observations of ganglionic *Hro-eve* expression were made at stage 10, whereas scoring for serotonergic neurons and segmental nerve formation was carried out at stage 11. Together, these results suggest that AS-*Hro-eve* MO injections resulted in a widespread failure of neural development at some point prior to terminal differentiation. Consistent with the fact that *Hro-eve* is expressed in all five teloblast lineages in early development, the defects induced by AS-*Hro-eve* MO injections were not restricted to neuronal tissues. For example, the O lineage normally makes a mixture of neurons and epidermal cells (Fig. 8G). Here, AS-*Hro-eve* MO injections resulted in an almost total loss of epidermal cells; neural precursors could be recognized by their ganglionic locations, but as in the N lineage, failed to complete differentiation (Fig. 8H).

Injection of antisense *Hro-eve* oligonucleotide disrupted the normal pattern of teloblast and blast cell divisions

To investigate the origins of the hairpin loops that occurred in the experimental side of germinal plates, we further examined embryos in which N teloblasts were injected with AS-*Hro-eve* MO or MM-*Hro-eve* MO as above, but fixed earlier, at mid stage 8 (~42-48 hours after the injection). At this stage, control germinal bands reached smoothly around the equator of the embryo, as in uninjected embryos (Fig. 10). By contrast, germinal bands on the experimental side often exhibited a prominent dorsally directed kink in the posterior part of the germinal band (Fig. 10).

Did the kinked germinal bands result from elongated n bandlets, reflecting increased rates of cell division in the teloblasts and/or primary blast cells? To address this possibility, embryos in which the N teloblasts had been injected with AS-*Hro-eve* MO or MM-*Hro-eve* MO were fixed at late stage 7 (24 hours after the injection) to examine the divisions of teloblast and primary blast cells in segmentation. At this stage, most of the primary blast cells still lie beneath the surface of the embryo; therefore, cell division patterns in labeled bandlets were reconstructed from sectioned embryos, making use of the facts that the teloblast cell cycle is ~50 minutes long at 23°C in *H. robusta* and that the primary blast cells remain in coherent bandlets. Thus, the most recently produced blast cells lie next to the teloblast and older clones lie progressively more distal within the bandlet. Moreover, in normal development, the nf and ns blast cells exhibit prolonged cell cycles (~26 hours and ~28 hours, respectively), then both undergo distinct, but stereotyped patterns of cell divisions; the first division is slightly unequal in both nf and ns (Fig. 1) (Bissen and Weisblat, 1989; Zackson, 1984) and takes place within ~6 hours of the cells entering the germinal band. It is possible to identify those clones that have undergone their first division by the size differences of the cells and nuclei within the bandlet.
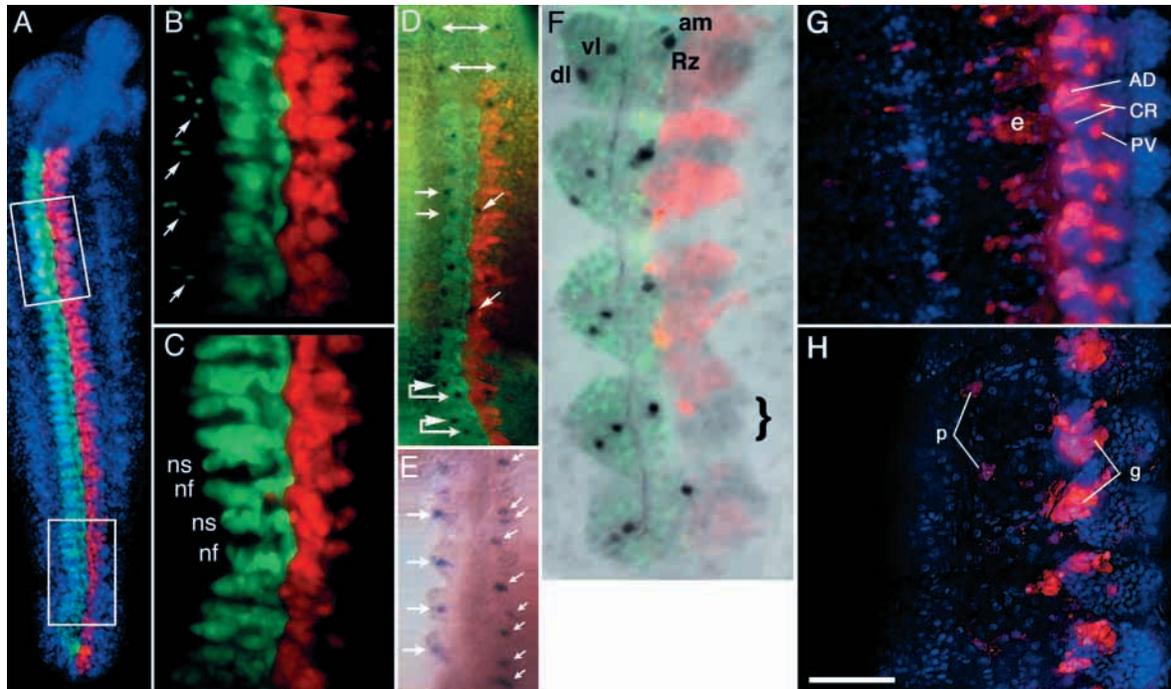
Fig. 8. Injection of AS-*Hro-eve* MO into N lineage perturbs gangliogenesis and neuronal differentiation (anterior is upwards). (A-C) Fluorescence images of the dissected germinal plate from a stage 10 embryo, in which one N teloblast had been co-injected with MM-*Hro-eve* MO and FDA (green), and the other with AS-*Hro-eve* MO and RDA (red) at early stage 7; nuclei are counterstained with Hoechst 33258 (blue). (B,C) Close-up views of the sections indicated by boxes in the anterior and posterior regions of A, respectively. On the control side (left), development of the N lineage is normal; peripheral nz neurons (derived from the nf blast cell clones) are present in anterior segments (arrows in B), and anterior and posterior lobes of cells (derived from ns and nf, respectively) that form the bulk of the ganglionic primordia are visible in posterior segments (C). On the experimental (right) side, the overall size and regularity of the n-derived clones are reduced and nz neurons are largely absent. (D) Fluorescence image of a preparation as in A, but processed for *Hro-eve* transcripts at stage 10. Two anterior ganglia, containing n blast cell clones produced prior to the injections, show bilaterally paired posterior spots of cells expressing *Hro-eve* (double arrows). On the control (left) side, these spots continue with segmental periodicity for a total of 14 segments (horizontal arrows; the spot in the third segment is out of focus); in the three youngest segments, the transient, anterior spots of *Hro-eve* expression are also visible on the control side (e.g. yoked arrowheads and arrows). On the experimental side, spots of *Hro-eve* expression are frequently missing, out of register, or misplaced medially with respect to those on the control side (slanted arrows). (E) Brightfield (Nomarski optics) showing approx. five ganglia from another embryo, treated as in D. Note the abnormal ganglion morphology and ectopically positioned *Hro-eve* spots (slanted arrows) on the experimental (right) side relative to the control side (horizontal arrows). (F) Combined bright-field and fluorescence image, showing the first five midbody ganglia (M1-M5) of an embryo injected as in A, but grown to stage 11 and processed for serotonergic neurons, which normally arise in bilateral pairs from the N teloblast lineages. No serotonergic neurons arose from the N teloblast injected with AS-*Hro-eve* MO and there is a gap (bracket) in the RDA-labeled lineage where N-derived neurons are missing. In M1-M5 of the control side (left), previously described serotonergic neurons (Stuart et al., 1987) can be identified, including the Retzius cells (Rz) and a pair of dorsolateral and ventrolateral cells (dl/vl). Ganglia M1-M3 also contain a smaller anteromedial (am) neuron. A fourth, posteromedial neuron was not detected because it develops later. (G) Digital montage fluorescence image combining several focal planes of five segments from a stage 11 embryo, in which an O teloblast had been injected with RDA and MM-*Hro-eve* MO at stage 7; in each segment, the O lineage generates distinct subsets of ganglionic neurons (AD, PV, CR), epidermal cells (e), plus peripheral neurons (most of which are not visible in this figure). (H) Equivalent view of a sibling embryo to that shown in G, that had been injected with AS-*Hro-eve* MO; clusters of undifferentiated cells are present over the ganglion (g) and in the periphery (p). Scale bar: 200 μm in A; 50 μm in B,C,F; 150 μm in D; 100 μm in E,G,H.

This normal pattern was observed in bandlets derived from N teloblasts injected with MM-*Hro-eve* MO or with lineage tracer alone. Each control bandlet contained between 26 and 28 clones and, with two exceptions, the blast cells were labeled uniformly throughout each bandlet (Fig. 11). Of the two exceptional bandlets, one contained a single blast cell with noticeably fainter lineage tracer than the others, while in the second bandlet 18 out of 28 cells were noticeably fainter. In all but one of the control bandlets, the oldest clone had undergone its unequal first mitosis (Fig. 12). In two of these bandlets, another blast cell had divided, giving an average of 1.1 mitoses per bandlet.

Bandlets derived from experimental N teloblasts contained about the same number of primary blast cell clones as did controls, indicating that the cell cycle duration of the teloblast was not affected (Fig. 12). However, the experimental bandlets differed from controls in two respects. First, the division pattern of the blast cells was disrupted, in that there were more clones in each bandlet that had already undergone mitosis (an average of 2.1 per bandlet) than in control bandlets. Moreover, the two-cell clones were not confined to the distal ends of the bandlet, indicating that some cells had divided much earlier than normal. Second, the bandlets invariably comprised an irregular sequence of brightly and faintly labeled blast cells
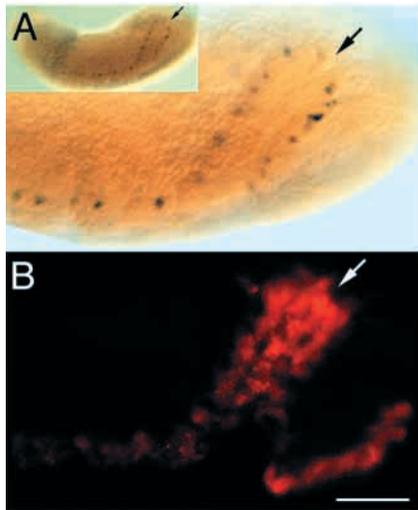
Fig. 9. Embryos with severe AS-*Hro-eve* MO phenotype produce hairpin loops in germinal plate. (A) Bright-field image showing a lateral view (ventral is downwards, anterior towards the left) of the posterior portion of an embryo in which an N teloblast had been injected with AS-*Hro-eve* MO and RDA at early stage 7; the embryo was processed for ganglionic *Hro-eve* expression at stage 10 (inset shows the whole embryo). Note that the pattern of *Hro-eve* positive spots demonstrates a prominent dorsal excursion (arrow). (B) Fluorescence image of the same specimen shows that the labeled bandlet contains a dorsally directed hairpin loop in this region (arrow indicates same point as in A). Scale bar: 50 µm in A,B; 175 µm in the inset.

(Figs 11, 12). One explanation for the variation is that the experimental teloblasts generate blast cells with variable proportions of yolk-rich and yolk-deficient cytoplasm (lineage tracer is largely excluded from yolk platelets), but we observed no difference in the cytoplasm of faintly labeled versus brightly labeled blast cells (data not shown). Two other possibilities are: (1) that the experimental teloblasts produce blast cells of varying volumes, and that the smaller cells then grow, diluting the inherited lineage tracer; or (2) that some blast cells are metabolically altered so that they secrete or sequester the lineage tracer. We have no evidence bearing on these possibilities, but in any case, injection of AS-*Hro-eve* MO had somehow disrupted the normal stem cell divisions in teloblasts. Thus, we conclude that injecting teloblasts with AS-*Hro-eve* MO perturbed cell divisions and fate decisions directly or indirectly throughout the subsequent development of the N lineage, beginning with the stem cell divisions of the teloblasts themselves.

DISCUSSION

In the work presented here, we identified *eve*-class genes, *Hro-eve* and *Ttr-eve*, from two species of glossiphoniid leeches. We have begun to characterize the expression and function of *Hro-eve* by semi-quantitative RT-PCR, in situ hybridization and injection of antisense MO.

Early expression of *Hro-eve*

In situ hybridization reveals that *Hro-eve* is expressed during
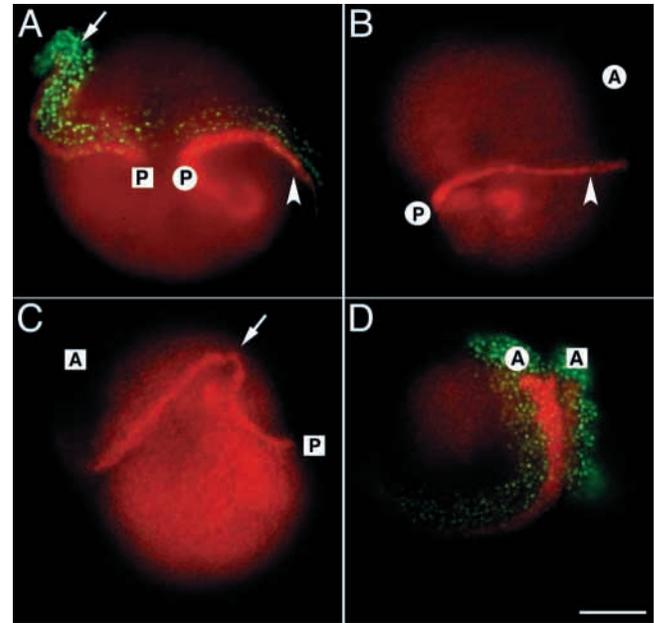

Fig. 10. Embryos with severe AS-*Hro-eve* MO phenotype produce kinked germinal bands. Fluorescence images of an embryo in which the left N teloblast had been injected with AS-*Hro-eve* MO and RDA (red), and the right N teloblast with generic control MO and RDA, at early stage 7. The resultant embryo was fixed and counterstained with Hoechst 33258 (pseudo-colored green in A and D); the animal pole (prospective dorsal) is upwards. (A) A roughly posterior (P) view of the embryo reveals the labeled n bandlets at the leading edges of the left and right germinal bands. While the control germinal band (circle, arrowhead) projects equatorially, the experimental germinal band (square, arrow) makes a marked dorsal deflection. (B) Lateral view of the right germinal band shows that it projects along the equator of the embryo. (C) Lateral view of the left germinal band shows the dorsally directed kink. (D) An obliquely ventral view shows the anterior (A) ends of the labeled bandlets within the partially formed germinal plate. The lineage tracer is brighter within the control bandlet, suggesting that the volume of the control injection was greater than that of the AS-*Hro-eve* MO injection. Scale bar: 100 µm.

cleavage and in all teloblast lineages up through the first division of the primary blast cells. No pair-rule or striped pattern is observed for *Hro-eve* during segmentation.

In teloblasts and primary blast cells, the in situ signal for *Hro-eve* is strongest over the chromatin of cells in mitosis. One interpretation of these results is that pre-existing *Hro-eve* transcripts localize to chromatin upon nuclear envelope breakdown during mitosis. An alternative explanation is that *Hro-eve* is transcribed during mitosis; in this case, the transcripts might remain associated with chromatin because the biochemical machinery required for splicing and polyadenylation is not operative during mitosis (Alberts et al., 1994). The generalization is sometimes made that transcription is shut down during mitosis, but this is not an absolute condition; in yeast, ~300 genes have been identified as being transcribed during mitosis (Krebs et al., 2000; Spellman et al., 1998).

Neuronal expression of *Hro-eve*

Semi-quantitative RT-PCR reveals that *Hro-eve* transcripts are

Fig. 11. Progeny of teloblasts injected with AS-*Hro-eve* MO exhibit dramatic variability in the brightness of inherited lineage tracer. Digital fluorescence images of an intact embryo (A) and a sectioned one (B,C) in which one N teloblast had been injected with MM-*Hro-eve* MO and FDA (green) and the other with AS-*Hro-eve* MO and RDA (red) at stage 7; the injected embryos were fixed and counterstained with Hoechst 33258 (blue) ~24 hours after the injections. Blast cells derived from teloblasts injected with MM-*Hro-eve* MO are uniformly labeled (A,B), whereas those derived from teloblasts injected with AS-*Hro-eve* MO exhibit marked cell-to-cell differences in the intensity (A,C). Scale bar: 50 μm.

Fig. 12. Injection of AS-*Hro-eve* MO disrupts the normal pattern of teloblast and blast cell divisions. Schematic summary of the analysis of labeled bandlets in sectioned embryos such as those depicted in Fig. 11. Each bandlet is represented by a row of rectangles, the color of which corresponds to the lineage tracer used (green, FDA; red, RDA). The parent teloblast (tb) would lie at the left end of each row; approximate ages of the blast cell progeny are indicated. Differences in lineage tracer intensity are indicated by brighter and darker shading. Blast cells that have undergone their first division are indicated by diagonal lines; question marks indicate a case in which we could not determine whether the cells indicated were two primary blast cells or sister cells derived from a single primary blast cell.

most abundant during the period in which ganglia are differentiating, and in situ hybridization reveals two sets of bilaterally paired, segmentally iterated neurons that express *Hro-eve* during neurogenesis. An anterior set of neurons, which are derived from the ns (probably from the ns.a) clone in each hemiganglion, expresses *Hro-eve* transiently, while a more posterior group of neurons, derived from the nf (probably from the nf.a) clone, continue to express *Hro-eve* in the oldest embryos studied (early stage 11).

Many genes that were first identified as regulating segmentation in *Drosophila* are also expressed later during neural development, including *even-skipped* (Doe et al., 1988; Frasch et al., 1987; Patel et al., 1989). The expression patterns of *eve*-class genes suggest similar dual functions in other arthropods (Damen et al., 2000; Patel et al., 1992). In nematodes (Ahringer, 1996), a taxon of unsegmented ecdysozoans, and in segmented deuterostomes, including amphibians (Ruiz i Altaba, 1990), fish (Thaeron et al., 2000) and mammals (Dush et al., 1992; Moran-Rivard et al., 2001), *eve* homologs are involved in neurogenesis. These results, together with our present findings, are consistent with the idea that *eve*-class genes functioned in neurogenesis in the last common ancestor of the deuterostomes, ecdysozoans and lophotrochozoans. However, we cannot yet rule out an alternative explanation for these observations, based on convergent evolution. In this scenario, the evolution of the many neuronal phenotypes present in higher metazoans entailed the independent recruitment to neuronal functions of transcription factors that were used for other purposes in ancestral animals. Further information on this issue may be gained by studying the function of *eve*-class genes from cnidarians (Finnerty and Martindale, 1997; Miles and Miller, 1992).
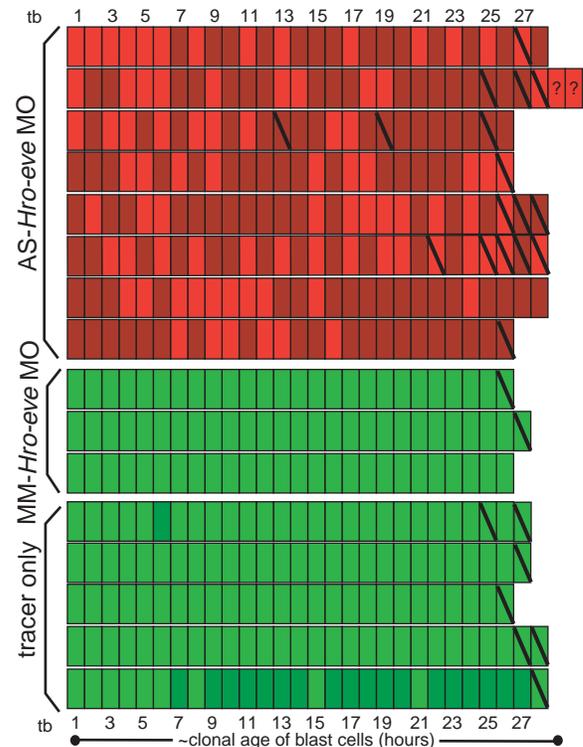
Developmental role of *Hro-eve* expression

The expression of *Hro-eve* in the early embryos, including the teloblasts and primary blast cells (segmental founder cells) of all five lineages (M, N, O, P and Q) suggests the possibility that this gene is somehow linked to the general regulation of cell proliferation, but not the specification of teloblast lineages or segment identity.

Evidence for the function of *Hro-eve* in the early *Helobdella* embryo was obtained by knockdown experiments, in which antisense oligonucleotides were injected into the N teloblasts, along with fluorescent lineage tracers to monitor the development of the injected cells. Lacking an antibody for *Hro-eve*, we are unable to measure the extent of the resulting knockdown, but do observe disruptions of normal development, beginning with teloblast and primary blast cell divisions. AS-*Hro-eve* MO injections do not affect the average rate or general asymmetry of the teloblast divisions, but the blast cells produced by the experimental teloblasts show variations in lineage tracer content that are not seen in control MO injections. Moreover, primary blast cells produced by the N teloblasts injected with AS-*Hro-eve* MO sometimes divided several hours earlier than normal, and

germinal bands containing bandlets derived from the experimental N teloblasts frequently exhibited a dorsally directed kink. We speculate that the kinks may result from mechanical deformations resulting from excess or ectopic N-derived cells that might be caused by the accelerated blast cell divisions, or from changes in biochemical properties that render these cells unable to undergo normal gastrulation movements.

The definitive fates of cells arising within the blast cell clones are also perturbed by AS-*Hro-eve* MO injections: there appear to be fewer than the normal number of cells; the usual groupings of cells within the hemiganglia are no longer evident; the three N-derived peripheral neurons in each hemisegment cannot be found. Neurons expressing *Hro-eve* are produced, but in ectopic positions compared with their contralateral homologs; by contrast, the serotonergic neurons that arise from the N teloblasts fail to differentiate.

Thus, we conclude that interfering with the expression of *Hro-eve* perturbs cell divisions of teloblasts and the subsequent divisions within the blast cell clones, consistent with the expression of *Hro-eve* in these cells during early development. The extent to which the effects on teloblasts and blast cells represent separate roles for *Hro-eve* remains to be determined.

Segmentation in annelids, arthropods and vertebrates

Until recently, the notion that segmentation is homologous between annelids and arthropods was generally accepted, as were phylogenetic trees in which variously defined clades of annelids and arthropods were placed as sister taxa. In addition to the segmentation per se, similarities between the posterior teloblastic growth zones in annelids and crustacean arthropods (Dohle and Scholtz, 1988) were taken as evidence supporting these assumptions. Logically, however, using phylogenetic trees based on developmentally derived traits as the reference framework for interpreting developmental comparisons introduces an inherent circularity to the process.

Molecular phylogenies, which offer a partial escape from this circularity, suggest that protostomes comprise distinct ecdysozoan and lophotrochozoan clades (Aguinaldo et al., 1997; Ruiz-Trillo et al., 1999) and that these have been separated since long before the Cambrian radiation (Adoutte et al., 2000). If so, given the paucity of segmented taxa among Ecdysozoa and Lophotrochozoa, it is more parsimonious to assume that segmentation has arisen independently in annelids and arthropods.

Consistent with this interpretation, work to date has revealed little similarity between the embryological functions of *Drosophila* segmentation genes and those of their homologs in *Helobdella*. For example, although it was initially concluded that *Helobdella engrailed*-class genes play an essential role in early segmentation (Ramirez et al., 1995; Wedeen and Weisblat, 1991), subsequent experimental analyses indicate that this is not the case (Seaver and Shankland, 1999; Seaver and Shankland, 2000; Shain et al., 1998; Shain et al., 2000). Also in contrast to *Drosophila*, the translation of maternally derived mRNA for the *Helobdella nanos*-class gene occurs after the AP axis is already established and correlates with the mesoderm-ectoderm fate decision (Pilon and Weisblat, 1997). In the work reported here, we find that *Hro-eve* is not expressed in a pair-rule pattern as in *Drosophila*. Moreover, we find no evidence of a link between the early expression of *eve*- and *engrailed*-class genes in leech. The early expression of *Hro-eve* shows no spatial or temporal correlation with that of *Hro-engrailed*.

eve-class genes are expressed in the posterior segmentation zone of annelids (Lophotrochozoa), arthropods (Ecdysozoa) and vertebrates (Deuterostomia) (Brown et al., 1997; Damen et al., 2000; Joly et al., 1993; Patel, 1994; Patel et al., 1992). One explanation for this similarity is that it reflects evolutionary convergence, i.e. independent recruitment of this transcription factor into the segmentation mechanisms in the three taxa. Alternatively, similarities in gene expression patterns between arthropods and vertebrates have led some to propose that the last common ancestor of all bilaterally symmetric animals was already segmented (De Robertis, 1997; Holland et al., 1997; Palmeirim et al., 1997). This latter explanation seems unlikely, on the basis of parsimony and, as reported here, because of the differences in the expression of *eve*-class genes between arthropods and leech.

REFERENCES

Adoutte, A., Balavoine, G., Lartillot, N., Lespinet, O., Prud'homme, B. and de Rosa, R. (2000). The new animal phylogeny: reliability and implications. *Proc. Natl. Acad. Sci. USA* **97**, 4453-4456.

Aguinaldo, A. M., Turbeville, J. M., Linford, L. S., Rivera, M. C., Garey, J. R., Raff, R. A. and Lake, J. A. (1997). Evidence for a clade of nematodes, arthropods and other moulting animals. *Nature* **387**, 489-493.

Ahringer, J. (1996). Posterior patterning by the *Caenorhabditis elegans* even-skipped homolog vab-7. *Genes Dev.* **10**, 1120-1130.

Alberts, B., Bray, D., Lewis, J., Raff, M., Roberts, K. and Watson, J. D. (1994). In *Molecular Biology of the Cell*. New York; Garland.

Bastian, H. and Gruss, P. (1990). A murine *even-skipped* homologue, *Evx 1*, is expressed during early embryogenesis and neurogenesis in a biphasic manner. *EMBO J.* **9**, 1839-1852.

Bissen, S. T. and Weisblat, D. (1987). Early differences between alternate n blast cells in leech embryo. *J. Neurobiol.* **18**, 251-270.

Bissen, S. T. and Weisblat, D. A. (1989). The durations and compositions of cell cycles in embryos of the leech, *Helobdella triserialis*. *Development* **106**, 105-118.

Blair, S. S. and Weisblat, D. A. (1984). Cell interactions in the developing epidermis of the leech *Helobdella triserialis*. *Dev. Biol.* **101**, 318-325.

Brown, S. J., Parrish, J. K., Beeman, R. W., Denell, R. E., Ruiz i Altaba, A. and Melton, D. A. (1997). Molecular characterization and embryonic expression of the *even-skipped* ortholog of *Tribolium castaneum*. *Mech. Dev.* **61**, 165-173.

Brusca, R. C. and Brusca, G. J. (1990). *Invertebrates*. Sunderland, MA; Sinauer.

Chen, Y. and Bissen, S. T. (1997). Regulation of *cyclin A* mRNA in leech embryonic stem cells. *Dev. Genes Evol.* **206**, 407-415.

Damen, W., Weller, M. and Tautz, D. (2000). Expression patterns of *hairy*, *even-skipped*, and *runt* in the spider *Cupiennius salei* imply that these genes were segmentation genes in a basal arthropod. *Proc. Natl. Acad. Sci. USA* **97**, 4515-4519.

Davis, G. K. and Patel, N. H. (1999). The origin and evolution of segmentation. *Trends Cell Biol.* **9**, M68-M72.

De Robertis, E. M. (1997). Evolutionary biology. The ancestry of segmentation. *Nature* **387**, 25-26.

Doe, C. Q., Hiromi, Y., Gehring, W. J. and Goodman, C. S. (1988). Expression and function of the segmentation gene *fushi tarazu* during *Drosophila* neurogenesis. *Science* **239**, 170-175.

Dohle, W. and Scholtz, G. (1988). Clonal analysis of the crustacean segment:

the discordance between genealogical and segmental borders. *Development* **104 Suppl.**, 147-160.

Duman-Scheel, M. and Patel, N. H. (1999). Analysis of molecular marker expression reveals neuronal homology in distantly related arthropods. *Development* **126**, 2327-2334.

Dush, M. K., Martin, G. R., Gutjahr, T., Patel, N. H., Li, X., Goodman, C. S. and Noll, M. (1992). Analysis of mouse *Evx* genes: *Evx-1* displays graded expression in the primitive streak. *Dev. Biol.* **151**, 273-287.

Faiella, A., D'Esposito, M., Rambaldi, M., Acampora, D., Balsofiore, S., Stornaiuolo, A., Mallamaci, A., Migliaccio, E., Gulisano, M., Simeone, A. et al. (1991). Isolation and mapping of *evx1*, a human homeobox gene homologous to *even-skipped*, localized at the 5′ end of HOX1 locus on chromosome 7. *Nucleic Acids Res.* **19**, 6541-6545.

Finnerty, J. R. and Martindale, M. Q. (1997). Homeoboxes in sea anemones (Cnidaria: Anthozoa): A PCR-based survey of Nematostella vectensis and Metridium senile. *Biol. Bull.* **193**, 62-76.

Frasch, M., Hoey, T., Rushlow, C., Doyle, H., Levine, M., Lall, S. and Patel, N. H. (1987). Characterization and localization of the even-skipped protein of *Drosophila*. *EMBO J.* **6**, 749-759.

Harland, R. M. (1991). In situ hybridization: An improved whole-mount method for *Xenopus* embryos. *Methods Cell Biol.* **36**, 685-695.

Holland, L. Z., Kene, M., Williams, N. A. and Holland, N. D. (1997). Sequence and embryonic expression of the amphioxus *engrailed* gene (AmphiEn): the metameric pattern of transcription resembles that of its segment-polarity homolog in Drosophila. *Development* **124**, 1723-1732.

Joly, J. S., Joly, C., Schulte-Merker, S., Boulekbache, H. and Condamine, H. (1993). The ventral and posterior expression of the zebrafish homeobox gene *eve1* is perturbed in dorsalized and mutant embryos. *Development* **119**, 1261-1275.

Kang, D., Pilon, M. and Weisblat, D. A. (2002). Maternal and zygotic expression of a *nanos*-class gene in the leech *Helobdella robusta*: primordial germ cells arise from segmental mesoderm. *Dev. Biol.* **245**, 28-41.

Kimmel, C. B. (1996). Was Urbilateria segmented? *Trends Genet.* **12**, 329-331.

Kramer, A. P. and Weisblat, D. A. (1985). Developmental neural kinship groups in the leech. *J. Neurosci.* **5**, 388-407.

Krebs, J. E., Fry, C. J., Samuels, M. L. and Peterson, C. L. (2000). Global role for chromatin remodeling enzymes in mitotic gene expression. *Cell* **102**, 587-598.

Macdonald, P. M., Ingham, P. and Struhl, G. (1986). Isolation, structure, and expression of *even-skipped*: a second pair-rule gene of *Drosophila* containing a homeo box. *Cell* **47**, 721-734.

Miles, A. and Miller, D. J. (1992). Genomes of diploblastic organisms contain homeoboxes: sequence of *eveC*, an *even-skipped* homologue from the cnidarian Acropora formosa. *Proc. R. Soc. Lond. B. Biol. Sci.* **248**, 159-161.

Moran-Rivard, L., Kagawa, T., Saueressig, H., Gross, M. K., Burrill, J. and Goulding, M. (2001). *Evx1* is a postmitotic determinant of v0 interneuron identity in the spinal cord. *Neuron* **29**, 385-399.

Nardelli-Haefliger, D. and Shankland, M. (1992). *Lox2* a putative leech segment identity gene is expressed in the same segmental domain in different stem cell lineages. *Development* **116**, 697-710.

Nasevicius, A. and Ekker, S. C. (2000). Effective targeted gene 'knockdown' in zebrafish. *Nat. Genet.* **26**, 216-220.

Ort, C. A., Kristan, W. B. and Stent, G. S. (1974). Neuronal control of swimming in the medicinal leech. *J. Comp. Physiol.* **94**, 121-154.

Palmeirim, I., Henrique, D., Ish-Horowicz, D. and Pourquie, O. (1997). Avian hairy gene expression identifies a molecular clock linked to vertebrate segmentation and somitogenesis. *Cell* **91**, 639-648.

Patel, N. H. (1994). Developmental evolution: insights from studies of insect segmentation. *Science* **266**, 581-590.

Patel, N. H., Ball, E. E. and Goodman, C. S. (1992). Changing role of even-skipped during the evolution of insect pattern formation. *Nature* **357**, 339-342.

Patel, N. H., Schafer, B., Goodman, C. S. and Holmgren, R. (1989). The role of segment polarity genes during Drosophila neurogenesis. *Genes Dev.* **3**, 890-904.

Pilon, M. and Weisblat, D. A. (1997). A nanos homolog in leech. *Development* **124**, 1771-1780.

Ramirez, F.-A., Wedeen, C. J., Stuart, D. K., Lans, D. and Weisblat, D. A. (1995). Identification of a neurogenic sublineage required for CNS segmentation in an Annelid. *Development* **121**, 2091-2097.

Ruiz i Altaba, A. (1990). Neural expression of the Xenopus homeobox gene *Xhox3*: evidence for a patterning neural signal that spreads through the ectoderm. *Development* **108**, 595-604.

Ruiz i Altaba, A. and Melton, D. A. (1989). Bimodal and graded expression of the Xenopus homeobox gene *Xhox3* during embryonic development. *Development* **106**, 173-183.

Ruiz-Trillo, I., Riutort, M., Littlewood, D. T., Herniou, E. A. and Baguna, J. (1999). Acoel flatworms: earliest extant bilaterian Metazoans, not members of Platyhelminthes. *Science* **283**, 1919-1923.

Seaver, E. C. and Shankland, M. (1999). Autonomous development during segment formation in leech: Evidence contradicting a role for *engrailed* as initiator of a signalling pathway in the segment primordium. *Dev. Biol.* **210**, 207.

Seaver, E. C. and Shankland, M. (2000). Leech segmental repeats develop normally in the absence of signals from either anterior or posterior segments. *Dev. Biol.* **224**, 339-353.

Shain, D. H., Ramirez-Weber, F.-A., Hsu, J. and Weisblat, D. A. (1998). Gangliogenesis in leech: Morphogenetic processes leading to segmentation in the central nervous system. *Dev. Genes Evol.* **208**, 28-36.

Shain, D. H., Stuart, D. K., Huang, F. Z. and Weisblat, D. A. (2000). Segmentation of the central nervous system in leech. *Development.* **127**, 735-744.

Smith, C. M. and Weisblat, D. A. (1994). Micromere fate maps in leech embryos: Lineage-specific differences in rates of cell proliferation. *Development* **120**, 3427-3438.

Spellman, P. T., Sherlock, G., Zhang, M. Q., Iyer, V. R., Anders, K., Eisen, M. B., Brown, P. O., Botstein, D. and Futcher, B. (1998). Comprehensive identification of cell cycle-regulated genes of the yeast *Saccharomyces cerevisiae* by microarray hybridization. *Mol. Biol. Cell* **9**, 3273-3297.

Stent, G. S., Kristan, W. B., Jr, Torrence, S. A., French, K. A. and Weisblat, D. A. (1992). Development of the Leech Nervous System. *Int. Rev. Neurobiol.* **33**, 109-193.

Stuart, D. K., Blair, S. S. and Weisblat, D. A. (1987). Cell lineage, cell death, and the developmental origin of identified serotonin- and dopamine-containing neurons in the leech. *J. Neurosci.* **7**, 1107-1122.

Thaeron, C., Avaron, F., Casane, D., Borday, V., Thisse, B., Thisse, C., Boulekbache, H. and Laurenti, P. (2000). Zebrafish *evx1* is dynamically expressed during embryogenesis in subsets of interneurones, posterior gut and urogenital system. *Mech. Dev.* **99**, 167-172.

Wedeen, C. J. and Weisblat, D. A. (1991). Segmental expression of an *engrailed*-class gene during early development and neurogenesis in an annelid. *Development* **113**, 805-814.

Weisblat, D. and Huang, F. (2001). An overview of glossiphoniid leech development. *Can. J. Zool.* **79**, 218-232.

Weisblat, D. A., Kim, S. Y. and Stent, G. S. (1984). Embryonic origins of cells in the leech *Helobdella triserialis*. *Dev. Biol.* **104**, 65-85.

Zackson, S. L. (1984). Cell lineage, cell-cell interaction, and segment formation in the ectoderm of a glossiphoniid leech embryo. *Dev. Biol.* **104**, 143-160.